

“Bottom up” strategy for the identification of novel soybean peptides with ACE-inhibitory activity

Luca Dellafiora¹, Raffaele Pugliese², Carlotta Bollati⁴, Fabrizio Gelain^{2,3}, Gianni Galaverna¹, Anna Arnoldi⁴, Carmen Lammi^{4*}

¹ Department of Food and Drug, University of Parma, Parma, Italy.

² Tissue Engineering Unit, Institute for Stem Cell Biology, Regenerative Medicine and Innovative Therapies- ISBReMIT, Fondazione IRCSS Casa Sollievo della Sofferenza, San Giovanni Rotondo (FG), Italy

³ Center for Nanomedicine and Tissue Engineering (CNTE), ASST Grande Ospedale Metropolitano Niguarda, Milan, Italy

⁴ Department of Pharmaceutical Sciences, University of Milan, Milan, Italy

*Corresponding author: Phone: +39-0250319372; Email: carmen.lammi@unimi.it.

1 Abstract

2 IAVPTGVA (Soy1) and LPYP are two soybean peptides, which display a multifunctional behavior
3 showing *in vitro* hypocholesterolemic and hypoglycemic activities. A preliminary screening of their
4 structures using BIOPEP suggested that they might be potential angiotensin converting enzyme
5 (ACE) inhibitors. Therefore, a bottom up-aided approach was developed in order to clarify the *in*
6 *vitro* hypotensive activity. Soy1 and LPYP dropped the intestinal and renal ACE enzyme activity
7 with IC₅₀ values equal to 14.7±0.28 μM and 5.0±0.28 μM (Caco-2 cells), and 6.0±0.35 and 6.8±0.20
8 μM (HK-2 cells), respectively. In parallel, a molecular modeling study suggested their capability to
9 act as competitive inhibitors of this enzyme. Finally, in order to increase both their stability and
10 hypotensive properties, a suitable strategy for the harmless control of their release from a
11 nanomaterial was developed through their encapsulation into the RADA16 assembling peptide.

12

13

14 **Keywords:** ACE, peptide encapsulation, bioactive peptides, hypotensive peptides, multifunctional
15 peptides, self-assembling peptides.

16

17 INTRODUCTION

18

19 Hypertension is one of the main risk factors for the development of cardiovascular diseases.¹ A
20 complex interaction of genetic and environmental factors as well as many other factors (i.e. increased
21 levels of long-term high sodium intake, inadequate dietary intake of potassium and calcium, elevated
22 renin-angiotensin system (RAS) activity, and endothelial dysfunction) are the basis of the
23 pathophysiological development of this disease.^{2, 3} In this context, angiotensin converting enzyme
24 (ACE, EC 3.4.15.1), a dipeptidyl-carboxypeptidase expressed in many tissues (lung, kidney,
25 intestine), is a key enzyme for blood pressure regulation, being responsible of the conversion of
26 inactive angiotensin I (Ang) into active Ang II, a vasoconstrictive octapeptide that is accountable for
27 the hypertension progression.⁴ The inhibition of this enzyme is therefore considered a successful
28 strategy for lowering high blood pressure.

29 This is also true in the field of hypotensive food peptides: indeed, several peptides from milk, meat,
30 egg, fish, lupin, and soybean sources have been singled out as inhibitors of the ACE activity.⁵⁻⁸ Milk
31 proteins have a leading role as a source of ACE inhibitory peptides: in particular, VPP and IPP, two
32 peptides deriving from β -casein and κ -casein, are the most active ACE-inhibitors from any food
33 source;⁹ their hypotensive effect has been confirmed *in vivo* in spontaneously hypertensive rats (SHR)
34 fed with sour milk and they are now on the market as ingredients of antihypertensive drinks, such as
35 the Japanese “Calpis” and the Finnish “Evolus”.¹⁰

36 IAVPTGVA (Soy1) and LPYP are peptides deriving from the hydrolysis of soybean glycinin with
37 pepsin and trypsin,¹¹ respectively, which have been demonstrated to be absorbable in Caco2 cell
38 monolayers.¹² More in detail, recent evidences suggest that both peptides are absorbed by
39 differentiated Caco-2 cells as a function of time and that Soy1 is better absorbed than LPYP after 2 h
40 of incubation in the apical side of monolayers.¹² Mature enterocytes represent the first physiological
41 barrier that bioactive food peptides encounter after ingestion, therefore their absorption is a dynamic
42 process which coexists with their metabolic degradation. In light of this observation, some evidences

43 underline that during its absorption, Soy1 (IAVPTGVA) is partially metabolized by active Caco-2
44 cells membrane peptidases in three breakdown fragments (AVPTGVA, IAVP, and IAV), which are
45 also absorbed in the same cellular system.¹²

46 Both peptides have a multifunctional behavior since *in vitro* they are either hypocholesterolemic or
47 hypoglycemic.¹²⁻¹⁵ The cholesterol lowering effect is due to the inhibition of 3-
48 hydroxymethylglutaryl coenzyme A reductase (HMGCoAR) and the subsequent activation of the
49 low-density lipoprotein receptor (LDLR) pathway. Moreover, these effects are accompanied by an
50 increase of the phosphorylation level of HMGCoAR on Ser 872 (the inactive form of HMGCoAR),
51 *via* the activation of the adenosine monophosphate-activated protein kinase (AMPK) pathway.¹³ The
52 capacity to modulate glucose metabolism and uptake is linked to the activation of the AMPK and
53 protein kinase B (Akt) pathways.¹⁴ The activation of Akt (phosphorylated at Ser 473) leads to the
54 inhibition of glycogen synthase kinase-3 β (GSK3), which in turn regulates the glycogen synthase
55 (GS) activity with a modulation of the hepatic glycogen formation. In parallel, the increased protein
56 levels of glucose transporter type 4 (GLUT4) and glucose transporter type 1 (GLUT1) determine an
57 increased attitude of HepG2 cells to clear extracellular glucose. In other experiments, Soy1 and LPYP
58 have been demonstrated to be also capable of inhibiting the activity of dipeptidyl peptidase-IV (DPP-
59 IV), another favorable effect for diabetes prevention.^{12, 15}

60 A preliminary screening of the structures of Soy 1 and LPYP using BIOPEP
61 (www.uwm.edu.pl/biochemia)¹⁶ suggested that they might be compatible with a potential behavior
62 as ACE inhibitors. Hence, the first objective of this work was an evaluation of their ACE-inhibitory
63 activity. Instead of using the traditional *in vitro* assay on the enzyme purified from rat or rabbit
64 (mostly used in literature), our experimentation was based on a cellular assay performed in human
65 intestinal Caco-2 and kidney HK-2 cells, which are among the cells that mostly express this enzyme
66 in the body. In parallel, a molecular modeling study was carried out to investigate their capability to
67 act as competitive inhibitors of ACE, in agreement with previous studies.¹⁷ The *in silico* study was
68 based on a structure-based modeling of both ACE domains (namely, the N-domain and C-domain)

69 including pharmacophoric analysis, docking simulations, rescoring procedures, and molecular
70 dynamics.

71 Lastly, since we have previously reported that self-assembling peptide-based nanogels (SAPs) are a
72 viable platform for targeting metabolic diseases with bioactive peptides,^{18,19} thanks to their bona fide
73 properties, well-ordered nanostructures, and biocompatibility; here we provide a smart delivery
74 coating system of Soy1 and LPYP by using RADA16 hydrogel (Ac-RADARADARADARADA-
75 CONH₂). The feasibility of this encapsulation strategy was assessed mainly by rheology, ThT binding
76 assay, spectroscopy assay (CD and ATR-FTIR), and release kinetic experiments.

77

78 **MATERIALS AND METHODS**

79 **Materials.** All reagents and solvents were from commercial sources. See “Supplementary
80 Information” for further details on materials and methods.

81

82 ***In vitro* digestion of Soy1 and LPYP.** Pepsin solution (4 mg/mL in NaCl) was added to Soy1 and
83 LPYP (100 μM) at a 1:100 enzyme to substrate ratio (pH 2.0). The digestion was conducted at 37 °C
84 for 90 min under continuous stirring, and then the pH was adjusted to 7.2 with 1 M NaOH in order to
85 inactivate the enzyme. Then, pancreatin (4 mg/mL in H₂O) was added at a 1:50 enzyme to substrate
86 ratio. After digestion at 37 °C for 150 min, the enzyme was inactivated by heating at 95 °C for 10
87 min. Further details regarding the analysis are available on “Supplementary Information”.

88

89 **Cell culture.** Caco-2 cells, obtained from Institut National de la Santé et de la Recherche Médicale
90 (INSERM, Paris), were routinely sub-cultured as previously described.¹⁸ HK2 from ATCC were
91 cultured using Dulbecco Minimum Essential Medium-F12 (DMEM-F12) containing 25 mM glucose,
92 4 mM stable L-glutamine, 100 U L⁻¹ penicillin, 100 μg L⁻¹ streptomycin, supplemented with 10%
93 heat-inactivated fetal bovine serum (FBS Hyclone Laboratories, Logan, UT, USA)

94

95 **ACE activity cell-based assay.** Soy1 and LPYP were tested on Caco-2 and HK2 cells (5×10^4 /well
96 in black 96-well plates) at 0.1-250.0 μ M concentration ranges or vehicle in growth medium for 24 h
97 at 37 °C. For 2D cell culture on RADA16-Soy1 and RADA-LPYP hydrogels, Caco-2 cells were
98 seeded on the surface of the above-mentioned hydrogels at the density of 5×10^4 /well. The next day,
99 The ACE inhibitory activity was measured using the ACE1 Activity Assay Kit (Biovision, Milpitas
100 Blvd., Milpitas, CA, USA) following the manufacture's protocol. See See "Supplementary
101 Informations" for further details on Acer activity cell-based assay.

102

103 ***In silico* modeling.** A molecular modeling approach was used to investigate the interaction of
104 peptides with the N- and C-domain of human ACE from a molecular perspective. In more detail, the
105 computational analysis relied on pharmacophoric modeling followed by docking simulations coupled
106 to rescoring procedures to assess the capability of peptides to fit the catalytic sites of both domains,
107 as previously reported.¹⁷ Then, a 50 nsec dynamic simulations study was applied to assess their
108 capability to persist therein. See "Supplementary Informations" for further details on molecular
109 modeling.

110

111 **Synthesis and purification of RADA16.** As we previously reported¹⁸ RADA16 molecule was
112 synthesized by fluorenylmethoxycarbonyl solid-phase peptide synthesis and purified by HPLC. The
113 purity of lyophilized peptide was tested by single quadrupole mass spectrometry using an Alliance-
114 3100 LC-MS. After lyophilization, RADA16 was dissolved at 1% (w/v) in distilled waters.

115

116 **Rheological measurement.** Rheological measurement was performed by an AR-2000ex Rheometer
117 (TA Instruments, New Castle, DE, USA) with a 20 mm acrylic truncated plate. All peptide samples
118 were tested at the concentration of 1% (w/v) and the sample stage was set to 25 °C. The storage
119 modulus was recorded as a function angular frequency (0.1-100 Hz) at a fixed strain of 1%.

120

121 **Thioflavin T (ThT) spectroscopy assay.** The propensity of assembled peptides to form cross- β fibril
122 structures were performed by using ThT binding assay, as previously described.¹⁸

123

124 **Circular dichroism (CD) spectroscopy assay.** CD spectra of peptide samples were recorded in
125 continuous scanning mode (190-300 nm) at 25 °C using Jasco J-810 (Jasco Corp., Tokyo, Japan)
126 spectropolarimeter. All spectra were collected using a 1 mm path-length quartz cell and averaged
127 over three accumulations (speed: 10 nm min⁻¹). A reference spectrum of distilled water was recorded
128 and subtracted from each spectrum. The estimation of the peptide secondary structure was achieved
129 by using a literature method.²⁰

130

131 **Fourier transform infrared spectroscopy (FT-IR) analysis.** Similar to our previous report,¹⁸ FT-
132 IR analysis was performed on peptides dissolved at a final concentration of 1% (w/v) in distilled
133 water. More details are available on “Supplementary Information”.

134

135 **Kinetic of Soy1 and LPYP peptide release from the nanogels.** The peptide leaking from the
136 nanogels as a function of time was measured dissolving the nanogels in PBS and measuring the
137 concentrations of released peptides after 60, 180, and 360 min of incubation by using a method
138 previously described.¹⁹ See “Supplementary Information” for further details on kinetic evaluation of
139 both peptides release.

140

141 **Cell viability test.** Caco-2 cells were seeded on the surface of RADA16-Soy1 and RADA-LPYP
142 hydrogels at the density of 5×10^4 /well and cultured for 6 days. Intestinal cell growth was qualitatively
143 evaluated collecting images using Zeiss Axioplan 2 microscope (Oberkochen, Germania). Finally,
144 MTT experiments were carried using method previously reported.²¹

145

146 **Statistically Analysis.** Statistical analyses were carried out by One-way ANOVA using Graphpad

147 Prism 6 (Graphpad, La Jolla, CA, USA). Values were expressed as means \pm s.d. of three independent
148 experiments, each experiment was performed in triplicate; p -values < 0.05 were considered to be
149 significant.

150

151 **RESULTS AND DISCUSSION**

152 **Soy1 and LPYP inhibit the *in situ* ACE activity on human intestinal Caco-2 and kidney HK-2** 153 **cells**

154 Their metabolic propensity to be degraded by peptidases, which are physiologically active along the
155 entire gastrointestinal tract, might dramatically influence the bioactivity of food peptides. Literature
156 provides many studies dealing with the assessment of food bioactive peptide stability to the simulated
157 gastric digestion.^{22, 23} In order to in-depth characterize the multifunctional behavior of Soy 1 and
158 LPYP, their stability toward the *in vitro* gastric digestion was assessed by using pepsin and pancreatin.
159 Figure 1 indicates that after co-digestion with these enzymes, LPYP and Soy1 are degraded by only
160 $28.5\pm 1.4\%$ and $27.7\pm 0.3\%$, respectively. These results highlight that both Soy1 and LPYP are
161 noteworthy stable to the *in vitro* gastric digestion.

162 Based on these results, in order to investigate the potential hypotensive effect of Soy1 and LPYP,
163 their ability to drop *in situ* the ACE activity was evaluated by using a cell-based assay. In particular,
164 Caco-2 and HK-2 cells (5×10^4 /well) were treated with Soy1 and LPYP (0.1 - $250 \mu\text{M}$) over night. The
165 following day, cells were lysated and the ACE activity was measured directly in the cell lysates using
166 a fluorescent ACE substrate: in this assay the fluorescent signal is proportional to the enzyme activity.
167 As shown in Figure 2, Soy1 and LPYP reduced the enzyme activity with a dose-response trend in
168 both biological systems (Caco-2 and HK-2 cells). In particular, Soy 1 and LPYP displayed calculated
169 IC_{50} values equal to 14.7 ± 0.28 and $5.0\pm 0.28 \mu\text{M}$ in Caco-2 cells, respectively (Figure 2A); whereas,
170 the same peptides showed IC_{50} values equal to 6.0 ± 0.35 and $6.8\pm 0.20 \mu\text{M}$ in HK-2 cells, respectively
171 (Figure 2B).

172 Literature provides many examples of studies in which different food-derived peptides target the *in*
173 *vitro* activity of ACE. In all these studies, their biochemical characterization has been carried out
174 using *in vitro* tests employing the purified recombinant ACE enzymes from different animal species,
175 such as pig and rabbit. Although the ACE sequence is highly conserved among species,²⁴ the only
176 use of biochemical tools involving the purified ACE enzymes and a standard substrate provide only
177 an insufficient characterization of the activity before performing expensive *in vivo* experimental
178 studies. On the contrary, a cell-based assay is certainly more helpful, since it allows the investigation
179 of the enzyme in its natural environment and to account for possible metabolic modifications of the
180 peptide structure and activity. For this reason, two cellular systems, human intestinal Caco-2 and
181 renal HK-2 cells, were chosen to characterize the potential inhibitory activity of Soy1 and LPYP in a
182 more realistic way. In particular, the intestine is the first physiological barrier that peptides from food
183 sources encounter after ingestion and it is well known that intestine and kidney express high level of
184 ACE enzyme, where the ACE and RAS systems play a key role in the blood pressure regulation.^{25, 26}
185 Our findings clearly suggest that both soybean peptides show an outstanding ACE inhibitory activity:
186 LPYP displays comparable IC₅₀ values in Caco-2 and HK-2 cells, whereas Soy1 is 2-fold more active
187 at renal than intestinal level. This may be explained by the propensity of Soy1 to undergo a metabolic
188 degradation by active peptidases that are expressed in the apical side of intestinal cells. Indeed, a
189 recent study has demonstrated that intestinal cells absorb both LPYP and Soy 1, but during this
190 process, the latter is partially cleaved into shorter peptides (AVPTGVA, IAVP, and IAV).¹²
191 It is well recognized that soybean proteins contain many bioactive peptides exerting multiple health
192 benefits, i.e. hypocholesterolemic, anti-diabetic, anti-tumor, and hypotensive activity. In this context,
193 LAIPVNKP and LPHF are two ACE inhibitors reported in literature with IC₅₀ values of 70 and 670
194 μM, respectively.²⁷ Moreover, after the hydrolysis of soybean proteins with pepsin, five peptides have
195 been identified showing *in vitro* and *in vivo* hypotensive activity. In particular, IA shows an IC₅₀ value
196 of 153 μM, YLAGNQ (14 μM), FFL (37 μM), IYLL (42 μM), and VMDKPQG (39 μM). Their blood
197 pressure lowering activity has been also confirmed *in vivo* on SHR models.²⁸ Moreover, peptides

198 SPYP and WL, obtained from the hydrolysis of soybean glycinin by acid proteinase from *Monascus*
199 *purpureus*, have been shown to be able to inhibit the ACE activity *in vitro* with IC₅₀ values equal to
200 850 μM and 65 μM, respectively.²⁷ Surprisingly among the known ACE inhibitory peptides from
201 soybean proteins, SPYP and LPYP are very similar, the only difference relating to a single amino
202 acid residue. LPYP is 170-fold more potent than SPYP, suggesting that the presence of a hydrophobic
203 amino acid residue with an aliphatic chain (Leu) instead of a polar residue with a hydroxymethyl
204 group (Ser) leads to an impressive potency gain.

205 Since the literature on ACE inhibitory peptides from food is very extensive, a correlation between
206 their physico-chemical and structural properties with bioactivity is well established. In particular, to
207 produce ACE inhibition, hydrophobic peptides (2-8 amino acid residues) should contain in the N-
208 terminal hydrophobic amino acids, especially those with aliphatic chains such as Gly, Ile, Leu, and
209 Val, and at the C-terminal amino acids with cyclic or aromatic rings (Pro, Tyr, Trp).^{29, 30} Many
210 peptides derived from food proteins contain Pro at the C-terminal, a rule concerning mostly short
211 peptides.³¹ The ACE inhibitory activity is furthermore improved by the simultaneous occurrence of
212 a C-terminal Pro and an N-terminal branched-side aliphatic amino acid. Indeed, our results are in
213 agreement with these structure-activity relationships. In light of all these observations and in order to
214 get an insight of the binding mode of both peptides with the ACE enzyme, *in silico* investigations were
215 performed.

216

217 **Molecular modeling studies**

218 Soy1 and LPYP underwent a molecular modeling study in order to investigate their possible
219 interaction with the N- and C-domain of human ACE at a molecular level. The *in silico* study
220 consisted in the pharmacophoric description of both the catalytic sites of ACE, followed by docking
221 simulations coupled to rescoring procedures to better evaluate the protein-peptide interaction, in
222 agreement with previous studies.^{32,33} The top scored docking pose in each domain was then compared
223 with the respective pharmacophoric fingerprint providing a qualitative structure-activity relationship

224 analysis. Finally, LPYP, which showed the best IC₅₀ value and the highest computational scores (*vide*
225 *infra*), underwent 50 nanoseconds molecular dynamic simulations to study the geometrical stability
226 of its interaction over time.

227 As previously reported, the two catalytic sites showed a largely conserved sequence identity and a
228 similar spatial organization of residues, determining a comparable pocket shape and a similar
229 distribution of pharmacophoric properties.¹⁷ Concerning the results of docking simulations and re-
230 scoring procedures, LPYP but not Soy1 seemed able to favorably interact with the two catalytic sites
231 of ACE. Indeed, on one side, LPYP recorded a HINT score of 2570 and 2830 within the N- and C-
232 domain, respectively. On the other side, Soy1 recorded a HINT score of 20 and -374 within the N-
233 and C-domain, respectively. Notably, HINT score relates to the free energy of binding and,
234 specifically, the higher the score the stronger the interaction. Conversely, negative scores, as well as
235 scores proximal to zero, may indicate the lack of appreciable interaction, as previously reported.^{32, 34,}
236 ³⁵ On this basis, the capability of Soy1 to interact with the two catalytic sites was judged less favorable
237 than the one of LPYP.

238 The docking analysis poses of LPYP in each ACE catalytic site in respect to their respective
239 pharmacophoric fingerprints provided a molecular rationale to such results. As shown in Figure 3,
240 LPYP engaged both sites *via* a multiple hydrogen bonds network starkly complying with the
241 pharmacophoric fingerprint of the two pockets. Conversely, the N-terminal residues of Soy1 were
242 found not fully matching neither of the two catalytic sites, though the peptide could form hydrogen
243 bonds with its C-terminal residue. Specifically, both hydrophobic-polar and acid-acid interferences
244 were found, as shown in Figure 3B and 3D. These evidences provided a structural rationale explaining
245 the diverse scores recorded by LPYP and Soy1, pointing out the better capability of the former to
246 interact with the catalytic sites of ACE. The low compliance of Soy1 to the catalytic sites of ACE
247 eventually suggested its presumably low capability to inhibit ACE *via* a competitive mechanism with
248 the catalytic site. Nonetheless, this result was in apparent contrast with the experimental evidences
249 reported above stating its ACE inhibitory activity, though of a lower intensity than LPYP. However,

250 ACE inhibitory peptides may also interact in regions other than the catalytic sites changing the
251 capability of substrates to reach the catalytic core.³⁶ Therefore, Soy1 might act through mechanisms
252 that do not require the competitive binding at the catalytic sites.

253 Considering that Soy1 may be hydrolyzed by cells releasing fragments such as AVPTGVA, IAVPT
254 and IAVP¹², these fragments were also submitted to the docking and rescoring procedure to assess
255 their possible capability to fit the catalytic sites of ACE. AVPTGVA, IAVPT, and IAVP recorded
256 52, 50, and 1956 HINT scores within the N-domain, respectively. Conversely, they recorded 793,
257 624, and 2164 HINT scores within the C-domain, respectively. In particular, IAVP markedly
258 complied the pharmacophoric requirements of both pockets strongly retracing the mode of binding
259 of LPYP (Figure 3). Moreover, on the basis of the obtained scores, AVPTGVA and IAVPT were
260 found to better satisfy the pocket requirements of the C-domain than those of the N-domain (wherein
261 their interaction was considered not favored due to the low scores recorded). These results might
262 point to their possible preferential interaction and inhibition with the N-domain. This feature might
263 deserve future investigations in order to identify domain-specific inhibitory peptides.

264 Overall, these results support the full compliance of LPYP as ACE inhibitor *via* competitive
265 mechanisms at the catalytic sites of ACE. Conversely, the capability of Soy1 to interact with the
266 catalytic sites was judged less favored than that of LPYP. However, other non-competitive
267 mechanisms could not be excluded. In addition, Soy1 fragments released by cell peptidases might
268 competitively inhibit ACE concurring to the overall inhibitory potential of Soy1.

269 Finally, LPYP, which recorded both the best IC₅₀ in experimental trials and the highest scores in
270 computational analysis, was submitted to molecular dynamic simulations (50 nanoseconds) to check
271 the capability to persist within the catalytic sites of ACE over time. The interaction of LPYP was
272 found geometrically stable in both ACE domains, as shown by the low RMSD fluctuations of C-alpha
273 (Figure 3G). In addition, the inspection of LPYP trajectories revealed its persistence and stability
274 within both the catalytic sites (Figure 3H), further supporting its capability to inhibit ACE *via*
275 competitive mechanisms.

276

277 **Supramolecular approach for the development of Soy1 and LPYP based nanogels: mechanical,**
278 **structural and biological characterizations**

279 SAPs are a promising class of supramolecular nanomaterials for controlled drug delivery applications
280 and beyond. Here we report the feasibility of encapsulating the bioactive peptides Soy1 and LPYP
281 (Figure 4A-B) into self-assembly peptide RADA16.³⁷

282 In order to assess the ability of RADA16 to support the slow release of both Soy1 and LPYP peptide,
283 a 1% (w/v) of RADA16-Soy1 or RADA16-LPYP nanogels were prepared to characterize their
284 viscoelastic properties. Rheological measurements were performed to estimate the elastic response
285 (G') of nanogels, by varying frequencies of applied oscillatory stress at constant strain (0.1-100 Hz,
286 1% strain). All preassembled solutions showed typical soft hydrogel profiles,¹⁹ featuring a G' modulus
287 of ~1800 Pa and ~1100 Pa for RADA16-Soy and RADA16-LPYP respectively (Figure 4C).

288 The amyloidogenic nature of the nanogels was pursued using a Thioflavin T (ThT) binding assay
289 (Figure 4D). This assay enables evaluation of the amyloidogenic structures and cross- β fibril
290 formation of materials because β -rich structures feature ThT-binding sites. ThT assay resulted in high
291 fluorescence levels, as well as a typical amyloid-binding emission signal (peak at ~490 nm), thus
292 establishing the β -rich amyloidogenic nature of both nanogels. To study the secondary structure of
293 the nanogels in solution, CD spectroscopy was carried out. As expected, both nanogels exhibited a
294 CD signal comprising a negative peak near 215 nm and a positive peak at ~195 nm characteristic of
295 a β -sheet conformation (Figure 4E). To gain further information about the nanogels secondary
296 structure a literature method has been used,²⁰ which suggested that RADA16-Soy1 has 84% of β -
297 sheet structures, whereas RADA16-LPYP 78%. Thus, the CD spectra are in accordance with ThT
298 binding assay. Furthermore, the β -sheet structural arrangements of RADA16-Soy and RADA16-
299 LPYP were also supported by the ATR-FTIR spectroscopy (Figure 4F), which displayed two peaks
300 at ~1630 cm^{-1} and ~1695 cm^{-1} (Amide I region), and one peak centered around 1530 cm^{-1} (Amide
301 II region) typically associated with β -sheet signatures.

302 To investigate the capability of Soy1 and LPYP based nanogels to modulate the ACE activity, *in situ*
303 experiments were carried out on human intestinal Caco-2 cells (Figure 5A-D). Briefly, a total of
304 5×10^4 /well Caco-2 cells were seeded directly on top of the coating-nanogels in which Soy1 and LPYP
305 peptides had been entangled at the concentration of $1.0 \mu\text{M}$. Cells were cultured for 6 days in order
306 to evaluate the ability of both soybean peptide-based nanogels to act as cell culture coating. As shown
307 in Figure 5A, Caco-2 cells were able to grow on top of both coating-nanogels without significant
308 morphological variation compared to Caco-2 cells, which grew on top of the RADA16 hydrogel
309 alone. Indeed, as MTT results clearly suggested, no cytotoxicity effects were observed even after 6
310 days of cell culture (Figure 5B). After 6 days, Caco-2 cells are in a proliferative stage, they reach
311 confluence and even though, they are not fully differentiated in mature enterocytes, they express
312 enough amount of active membrane peptidases, i.e. DPP-IV and ACE.³⁸ For this reason, this cellular
313 system, which has already been used to monitor the *in situ* activity of DPP-IV, can be also utilized to
314 evaluate the ACE activity.^{39,40} Based on these results, the kinetic of each peptide release was assessed
315 using a literature method, which is based on chelating the peptide bonds by Cu (II) in alkaline media
316 and monitoring the change of absorbance at 330 nm.⁴¹ Using this method, it was demonstrated that
317 both peptides are released by the coating-hydrogel as a function of time with a different behavior. In
318 details, released Soy1 concentrations are 0.13 ± 0.04 , 0.27 ± 0.003 , and $0.51 \pm 0.08 \mu\text{g} \mu\text{L}^{-1}$, whereas
319 released LPYP peptide concentrations are 0.46 ± 0.04 , 0.84 ± 0.15 , $1.22 \pm 0.16 \mu\text{g} \mu\text{L}^{-1}$, respectively,
320 after 60, 180, and 360 min of incubation in PBS (Figure 5C). LPYP peptide is faster released than
321 Soy1 probably because it is less hydrophobic (LPYP hydrophobicity is equal to $6.22 \text{ Kcal mol}^{-1}$, and
322 that of Soy 1 is equal to $8.40 \text{ Kcal mol}^{-1}$). This explains why LPYP may more easily leak from the
323 entangled nanofibrous domains of the hydrogels than Soy1.

324 Further, the ability of both coating-nanogels to inhibit the ACE activity was evaluated *in situ* on
325 human intestinal Caco-2 cells. Findings clearly underline that both RADA16-Soy1 and RADA16-
326 LPYP maintain their ability to reduce the enzyme activity by 40% and 60%, respectively (Figure 5D).
327 In detail, when Soy1 and LPYP peptides are entrapped in the coating-nanogels at the concentration

328 of 1 μ M, they drop the ACE activity by $34.3\pm 7.6\%$ and $52.2\pm 3.8\%$, respectively, suggesting a clear
329 improvement of their inhibitory activity. These results are in agreement with the relative activity (data
330 not shown) of each peptide, i.e. LPYP is more active than Soy1. Overall, these results clearly support
331 our hypothesis of developing a suitable smart delivery coating-strategy for the harmless control of
332 ACE inhibitory peptides as a new approach for improving their activity and stability.

333

334 **Abbreviations**

335 **ACE**, angiotensin converting enzyme; **Akt**, protein kinase B; **AMC**, amido-4-methylcoumarin
336 hydrobromide; **AMPK**, adenosine monophosphate-activated protein kinase; **BB**, brush border; **CD**,
337 circular dichroism; **DMEM**, Dulbecco's modified Eagle's medium; **DPP-IV**, dipeptidyl peptidase-IV; **FBS**,
338 fetal bovine serum; **FT-IR**, Fourier transform infrared spectroscopy; **GLUT1**, glucose transporter type
339 1; **GLUT4**, glucose transporter type 4; **GS**, glycogen synthase; **GSK3**, glycogen synthase kinase-3 β ,
340 **HMGCoAR**, 3-hydroxymethylglutaryl coenzyme A reductase; **PBS**, phosphate buffered saline; **RAS**,
341 renin-angiotensin system; **RFU**, relative fluorescence unit; **RT**, room temperature; **SAPs**, self-assembling
342 peptides; **SHR**, spontaneous hypertensive rats; **TFA**, trifluoroacetic acid; **ThT**, Thioflavin T; **TIS**,
343 triisopropylsilane;

344

345 **Author Contributions**

346 C.L. conceived the project and designed the experiments. C.L. and C.B. took care all *in situ* and
347 release tests, L.D. performed in silico study, while R.P. and F.G synthesized the RADA16 peptide
348 and carried out all structural and biomechanical experiments. C.L., A.A, G.G., L.D, and R.P wrote
349 the manuscript. All authors critically reviewed the paper and have approved the final article.

350 **Acknowledgment**

351 We are indebted to Carlo Sirtori Foundation (Milan, Italy) for having provided part of equipment
352 used in this experimentation. This research also benefits from the HPC (high performance computing)

353 facility of the University of Parma, Italy. In addition, the authors would like to acknowledge Prof.
354 Gabriele Cruciani for the courtesy of FLAP software (www.moldiscovery.com) and Prof. Kellogg
355 and Prof. Cozzini for the courtesy of HINT.

356 **Supporting Information.** Supporting information provides a more detailed description of the
357 material & methods section. The Supporting Information is available free of charge on the ACS
358 Publications website at DOI: XXX.

359

360

361 **References**

- 362 1. Kjeldsen, S. E., Hypertension and cardiovascular risk: General aspects. *Pharmacol Res* **2018**,
363 *129*, 95-99.
- 364 2. Howell, S. J.; Sear, J. W.; Foëx, P., Hypertension, hypertensive heart disease and perioperative
365 cardiac risk. *Br J Anaesth* **2004**, *92* (4), 570-83.
- 366 3. Sarzani, R.; Salvi, F.; Dessì-Fulgheri, P.; Rappelli, A., Renin-angiotensin system, natriuretic
367 peptides, obesity, metabolic syndrome, and hypertension: an integrated view in humans. *J Hypertens*
368 **2008**, *26* (5), 831-43.
- 369 4. Zhuo, J. L.; Ferrao, F. M.; Zheng, Y.; Li, X. C., New frontiers in the intrarenal Renin-
370 Angiotensin system: a critical review of classical and new paradigms. *Front Endocrinol (Lausanne)*
371 **2013**, *4*, 166.
- 372 5. Ibrahim, H. R.; Ahmed, A. S.; Miyata, T., Novel angiotensin-converting enzyme inhibitory
373 peptides from caseins and whey proteins of goat milk. *J Adv Res* **2017**, *8* (1), 63-71.
- 374 6. Mora, L.; Gallego, M.; Toldrá, F., ACEI-inhibitory peptides naturally generated in meat and
375 meat products and their health relevance. *Nutrients* **2018**, *10* (9).
- 376 7. Auwal, S. M.; Zainal Abidin, N.; Zarei, M.; Tan, C. P.; Saari, N., Identification, structure-
377 activity relationship and in silico molecular docking analyses of five novel angiotensin I-converting
378 enzyme (ACE)-inhibitory peptides from stone fish (*Actinopyga lecanora*) hydrolysates. *PLoS One*
379 **2019**, *14* (5), e0197644.
- 380 8. Chatterjee, C.; Gleddie, S.; Xiao, C. W., Soybean bioactive peptides and their functional
381 properties. *Nutrients* **2018**, *10* (9).
- 382 9. Pripp, A. H., Effect of peptides derived from food proteins on blood pressure: a meta-analysis
383 of randomized controlled trials. *Food Nutr Res* **2008**, *52*.

- 384 10. Iwaniak, A.; Minkiewicz, P.; Darewicz, M., Food-originating ACE inhibitors, including
385 antihypertensive peptides, as preventive food components in blood pressure reduction. *Compr Rev*
386 *Food Sci F* **2014**, *13* (2), 114-134.
- 387 11. Pak, V. V.; Koo, M. S.; Kasymova, T. D.; Kwon, D. Y., Isolation and identification of peptides
388 from soy 11S-globulin with hypocholesterolemic activity. *Chem Nat Comp* **2005**, *41* (6), 710-714.
- 389 12. Aiello, G.; Ferruzza, S.; Ranaldi, G.; Sambuy, Y.; Arnoldi, A.; Vistoli, G.; Lammi, C.,
390 Behavior of three hypocholesterolemic peptides from soy protein in an intestinal model based on
391 differentiated Caco-2 cell. *J Funct Foods* **2018**, *45*, 363-370.
- 392 13. Lammi, C.; Zaroni, C.; Arnoldi, A., IAVPGEVA, IAVPTGVA, and LPYP, three peptides
393 from soy glycinin, modulate cholesterol metabolism in HepG2 cells through the activation of the
394 LDLR-SREBP2 pathway. *J Funct Foods* **2015**, *14*, 469-478.
- 395 14. Lammi, C.; Zaroni, C.; Arnoldi, A., Three peptides from soy glycinin modulate glucose
396 metabolism in human hepatic HepG2 cells. *Int J Mol Sci* **2015**, *16* (11), 27362-70.
- 397 15. Lammi, C.; Zaroni, C.; Arnoldi, A.; Vistoli, G., Peptides derived from soy and lupin protein
398 as Dipeptidyl-Peptidase IV inhibitors: *In vitro* biochemical screening and *in silico* molecular
399 modeling study. *J Agric Food Chem* **2016**, *64* (51), 9601-9606.
- 400 16. Minkiewicz, P.; Dziuba, J.; Darewicz, M.; Bucholska, J.; Mogut, D., Evaluation of In silico
401 prediction possibility of epitope sequences using experimental data concerning allergenic food
402 proteins summarised in BIOPEP database. *Pol J Food Nutr Sci* **2012**, *62* (3), 151-157.
- 403 17. Dellafiora, L.; Paoletta, S.; Dall'Asta, C.; Dossena, A.; Cozzini, P.; Galaverna, G., Hybrid in
404 silico/in vitro approach for the identification of angiotensin I converting enzyme inhibitory peptides
405 from parma dry-cured ham. *J Agric Food Chem* **2015**, *63* (28), 6366-75.
- 406 18. Lammi, C.; Bollati, C.; Gelain, F.; Arnoldi, A.; Pugliese, R., Enhancement of the stability and
407 anti-DPPiV activity of hempseed hydrolysates through self-assembling peptide-based hydrogels.
408 *Front Chem* 24 January 2019, <https://doi.org/10.3389/fchem.2018.00670>.

- 409 19. Pugliese, R.; Bollati, C.; Gelain, F.; Arnoldi, A.; Lammi, C., A supramolecular approach to
410 develop new soybean and lupin peptide nanogels with enhanced dipeptidyl peptidase IV (DPP-IV)
411 inhibitory activity. *J Agric Food Chem* **2019**, *67* (13), 3615-3623.
- 412 20. Raussens, V.; Ruyschaert, J. M.; Goormaghtigh, E., Protein concentration is not an absolute
413 prerequisite for the determination of secondary structure from circular dichroism spectra: a new
414 scaling method. *Anal Biochem* **2003**, *319* (1), 114-21.
- 415 21. Lammi, C.; Zanoni, C.; Scigliuolo, G. M.; D'Amato, A.; Arnoldi, A., Lupin peptides lower
416 low-density lipoprotein (LDL) cholesterol through an up-regulation of the LDL receptor/sterol
417 regulatory element binding protein 2 (SREBP2) pathway at HepG2 cell line. *J Agric Food Chem*
418 **2014**, *62* (29), 7151-9.
- 419 22. Hernández-Ledesma, B.; Miguel, M.; Amigo, L.; Aleixandre, M. A.; Recio, I., Effect of
420 simulated gastrointestinal digestion on the antihypertensive properties of synthetic beta-lactoglobulin
421 peptide sequences. *J Dairy Res* **2007**, *74* (3), 336-9.
- 422 23. Escudero, E.; Mora, L.; Toldrá, F., Stability of ACE inhibitory ham peptides against heat
423 treatment and in vitro digestion. *Food Chem* **2014**, *161*, 305-11.
- 424 24. Riordan, J. F., Angiotensin-I-converting enzyme and its relatives. *Genome Biol* **2003**, *4* (8),
425 225.
- 426 25. Bernstein, K. E.; Giani, J. F.; Shen, X. Z.; Gonzalez-Villalobos, R. A., Renal angiotensin-
427 converting enzyme and blood pressure control. *Curr Opin Nephrol Hypertens* **2014**, *23* (2), 106-12.
- 428 26. Naim, H. Y., Human small intestinal angiotensin-converting enzyme: intracellular transport,
429 secretion and glycosylation. *Biochem J* **1993**, *296* (Pt 3), 607-15.
- 430 27. Kuba, M.; Tana, C.; Tawata, S.; Yasuda, M., Production of angiotensin I-converting enzyme
431 inhibitory peptides from soybean protein with *Monascus purpureus* acid proteinase. *Process Biochem*
432 **2005**, *40* (6), 2191-2196.

- 433 28. Chen, J. R.; Okada, T.; Muramoto, K.; Suetsuna, K.; Yang, S. C., Identification of angiotensin
434 I-converting enzyme inhibitory peptides derived from the peptic digest of soybean protein. *J Food*
435 *Biochem* **2002**, *26* (6), 543-554.
- 436 29. FitzGerald, R. J.; Murray, B. A.; Walsh, D. J., Hypotensive peptides from milk proteins. *J*
437 *Nutr* **2004**, *134* (4), 980S-8S.
- 438 30. Vermeirssen, V.; Van Camp, J.; Verstraete, W., Bioavailability of angiotensin I converting
439 enzyme inhibitory peptides. *Br J Nutr* **2004**, *92* (3), 357-66.
- 440 31. Iwaniak, A.; Dziuba, J., Animal and plant proteins as precursors of peptides with ACE
441 inhibitory activity - An in silico strategy of protein evaluation. *Food Technol Biotech* **2009**, *47* (4),
442 441-449.
- 443 32. Dellafiora, L.; Marchetti, M.; Spyrakis, F.; Orlandi, V.; Campanini, B.; Cruciani, G.; Cozzini,
444 P.; Mozzarelli, A., Expanding the chemical space of human serine racemase inhibitors. *Bioorg Med*
445 *Chem Lett* **2015**, *25* (19), 4297-303.
- 446 33. Nongonierma, A. B.; Dellafiora, L.; Paoletta, S.; Galaverna, G.; Cozzini, P.; FitzGerald, R. J.,
447 Approaches applied to the study of peptide analogs of Ile-Pro-Ile in relation to their dipeptidyl
448 peptidase IV inhibitory properties. *Front Endocrinol (Lausanne)* **2018**, *9*, 329.
- 449 34. Eugene Kellogg, G.; Abraham, D. J., Hydrophobicity: is LogP(o/w) more than the sum of its
450 parts? *Eur J Med Chem* **2000**, *35* (7-8), 651-61.
- 451 35. Dellafiora, L.; Dall'Asta, C.; Cozzini, P., Ergot alkaloids: From witchcraft till. *Toxicol Rep*
452 **2015**, *2*, 535-545.
- 453 36. Ryan, J. T.; Ross, R. P.; Bolton, D.; Fitzgerald, G. F.; Stanton, C., Bioactive peptides from
454 muscle sources: meat and fish. *Nutrients* **2011**, *3* (9), 765-91.
- 455 37. Zhang, S.; Holmes, T.; Lockshin, C.; Rich, A., Spontaneous assembly of a self-
456 complementary oligopeptide to form a stable macroscopic membrane. *Proc Natl Acad Sci U S A* **1993**,
457 *90* (8), 3334-8.

- 458 38. Howell, S.; Kenny, A. J.; Turner, A. J., A survey of membrane peptidases in two human
459 colonic cell lines, Caco-2 and HT-29. *Biochem J* **1992**, *284* (Pt 2), 595-601.
- 460 39. Lammi, C.; Bollati, C.; Ferruzza, S.; Ranaldi, G.; Sambuy, Y.; Arnoldi, A., Soybean- and
461 lupin-derived peptides inhibit DPP-IV activity on in situ human intestinal Caco-2 cells and ex vivo
462 human serum. *Nutrients* **2018**, *10* (8).
- 463 40. Aiello, G.; Li, Y.; Boschin, G.; Bollati, C.; Arnoldi, A.; Lammi, C., Chemical and biological
464 characterization of spirulina protein hydrolysates: Focus on ACE and DPP-IV activities modulation.
465 *J Funct Foods*: 2019.
- 466 41. Goa, J., A micro biuret method for protein determination. Determination of total protein in
467 cerebrospinal fluid. *Scand J Clin Lab Invest* **1953**, *5*, 218-22.

468

469 **Funding**

470 The work was supported partially by Fondazione Cariplo, project “SUPER-HEMP: Sustainable
471 Process for Enhanced Recovery of Hempseed Oil”, code number 2017-1005, and partially by the
472 project ERA-NET SUSFOOD2: “DISCOVERY - Disaggregation of conventional vegetable press
473 cakes by novel techniques to receive new products and to increase the yield”.

474

475 **FIGURE CAPTIONS**

476 **Figure 1. *In vitro* gastrointestinal digestion.** LPYP (A) and Soy1 (B) were co-digested with pepsin for 90
 477 min and pancreatin for 150 min. After digestion, LPYP and Soy1 (D) were degraded by only $28.5\pm 1.4\%$ and
 478 $27.7\pm 0.3\%$, respectively vs undigested peptide (UD). Data represent the mean \pm s.d. of three independent
 479 experiments performed in triplicate

480

481 **Figure 2. *In situ* evaluation of the ACE activity.** Soy1 and LPYP reduce *in situ* the ACE activity with a
 482 dose-response trend (A) in non-differentiated human Caco-2 cells (IC_{50} values equal to 14.7 ± 0.28 and
 483 5.0 ± 0.28 μ M, respectively) and (B) in renal HK-2 cells (IC_{50} values equal to 6.0 ± 0.35 and 6.8 ± 0.20 μ M,
 484 respectively). Data represent the mean \pm s.d. of three independent experiments performed in triplicate.

485

486 **Figure 3. Molecular modeling results.** Protein is represented in cartoon, while peptides and residues involved
 487 in polar interactions are represented in sticks. Spheres represent Zn ions. Grey, red, and blue meshes indicate
 488 regions sterically and energetically favorable to receive hydrophobic, hydrogen bond acceptor, and hydrogen
 489 bond donor groups, respectively. Polar interactions are indicated by yellow dotted lines. The red and black
 490 circles indicate hydrophobic-polar and acid-acid interferences. (A) LPYP within C-domain. (B) Soy1 within
 491 C-domain. (C) LPYP within N-domain. (D) Soy1 within N-domain. (E) Superimposition of IAVP (yellow) to
 492 LPYP (purple) within C-domain. (F) Superimposition of IAVP (yellow) to LPYP (purple) within N-domain.
 493 (G) RMSD plots of LPYP within the catalytic site of C- and N-domain of ACE. (H) Time-step representation
 494 of LPYP trajectories within the N- and C-domain of ACE. The from-red-to-blue color switch indicates the
 495 stepwise changes of ligand coordinates over time (50 nanoseconds).

496

497 **Figure 4. Characterization of SAP-nanogels.** A) Cartoon representation and B) chemical structures of
 498 RADA16, RADA16-Soy 1 and RADA16-LPYP nanogels. C) Biomechanical characterization of RADA16-
 499 Soy1 and RADA16-LPYP nanogels via a frequency sweep test (0.1–100 Hz, 1% strain). D) ThT emission
 500 spectra of RADA16-Soy1 and RADA16-LPYP nanogels: their affinity for ThT may be ascribable to the
 501 presence of cross- β fibril structures. E) CD spectrum of RADA16-Soy1 and RADA16-LPYP in solution
 502 showing the presence of β -sheet assemblies. F) FTIR analysis of RADA16-Soy and RADA16-LPYP with

503 peaks at $\sim 1630\text{ cm}^{-1}$ and $\sim 1695\text{ cm}^{-1}$ (amide I region) and 1530 cm^{-1} (amide II region) typically associated
504 with β -sheet signatures.

505

506 **Figure 5. Biological characterization of the nanogels.** Photographs of the Caco-2 cells grown on top of
507 RADA, RADA-Soy1, and RADA-LPYP hydrogels for 6 days (A); cell viability tests performed by MTT assay
508 (B); kinetic of peptide release as a function of the time (C); evaluation of the *in situ* ACE-inhibitory effects on
509 human intestinal Caco-2 cells (D). Data represent the mean \pm s.d. of three independent experiments performed
510 in triplicate; **** $p < 0.0001$.

FIGURES

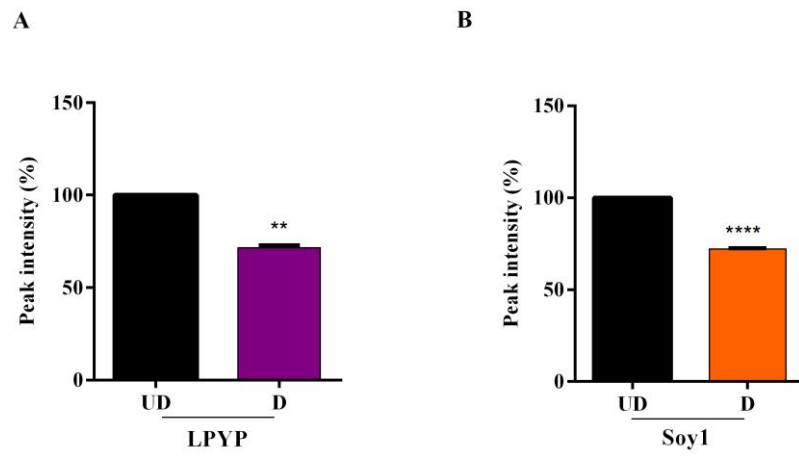
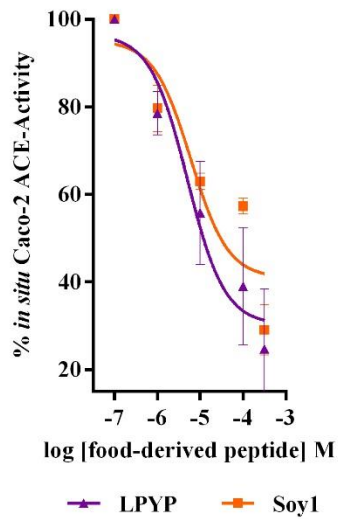


Figure 1

A



B

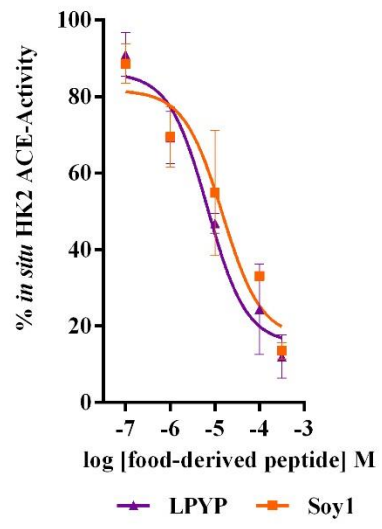


Figure 2

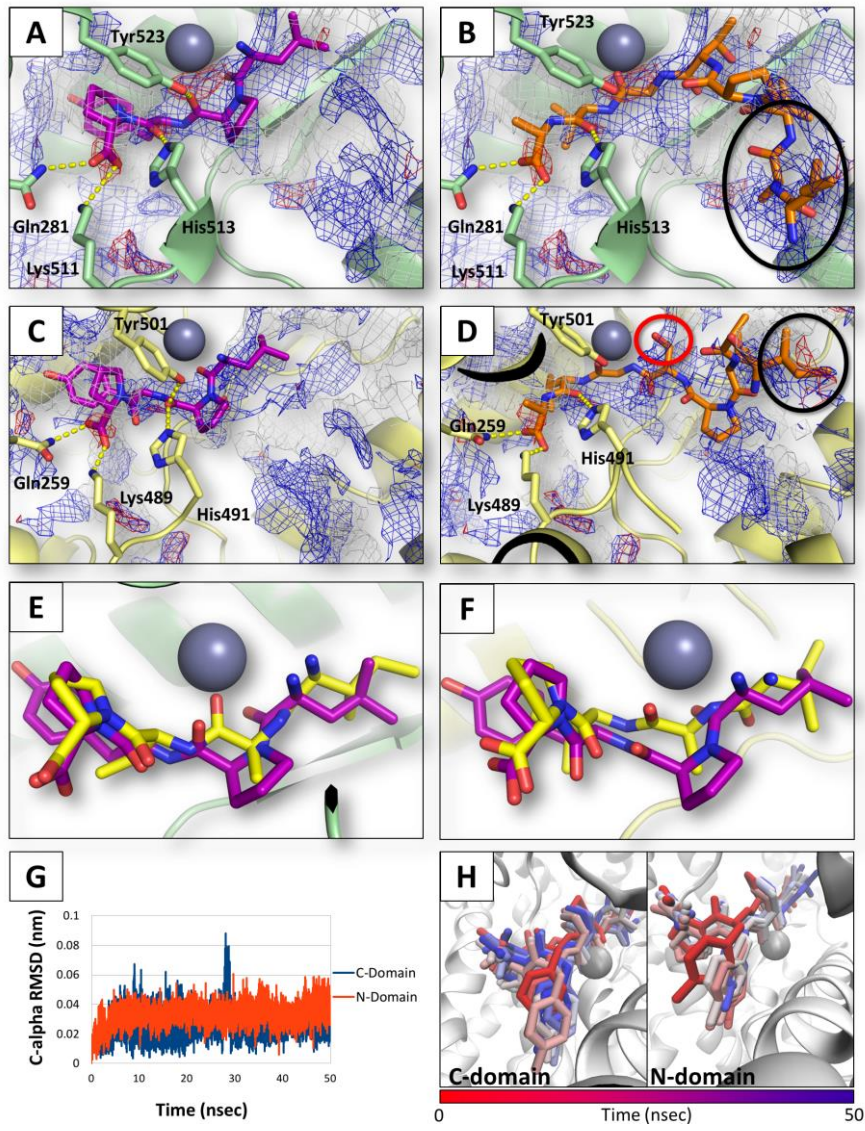


Figure 3

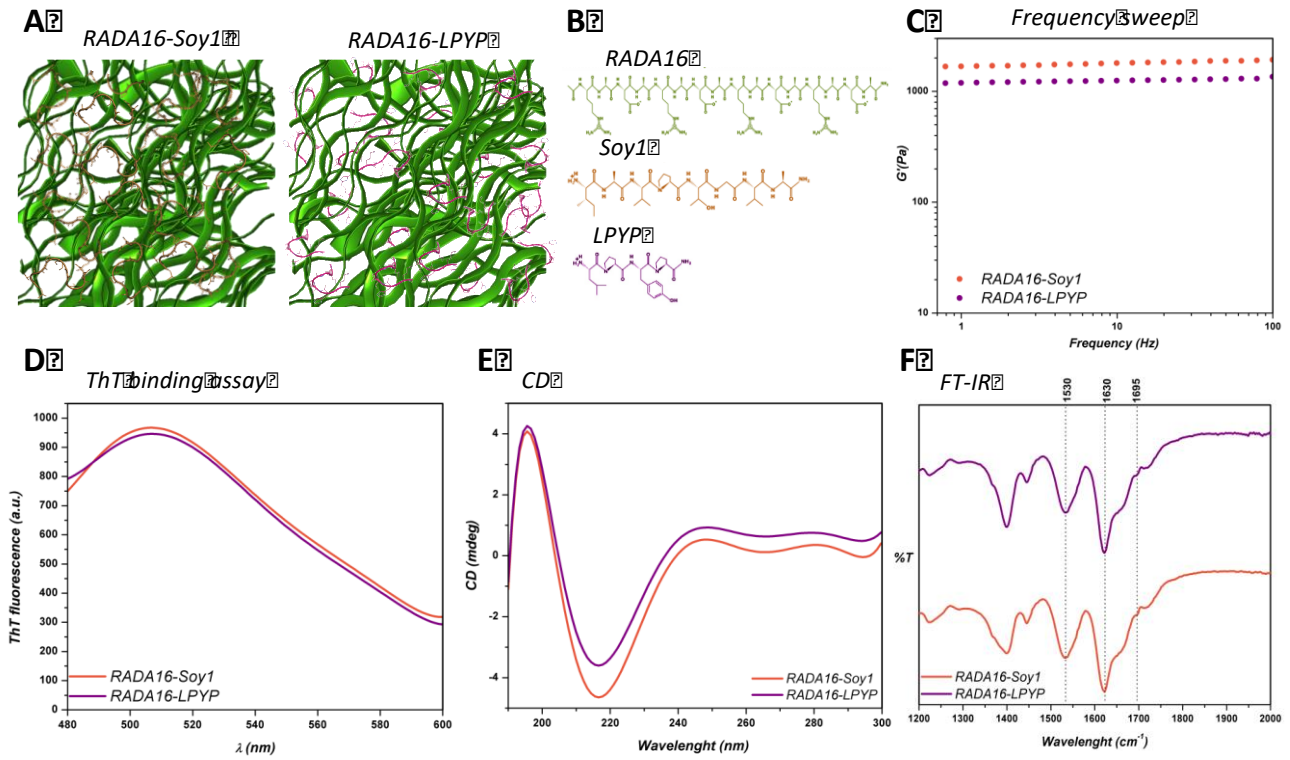


Figure 4

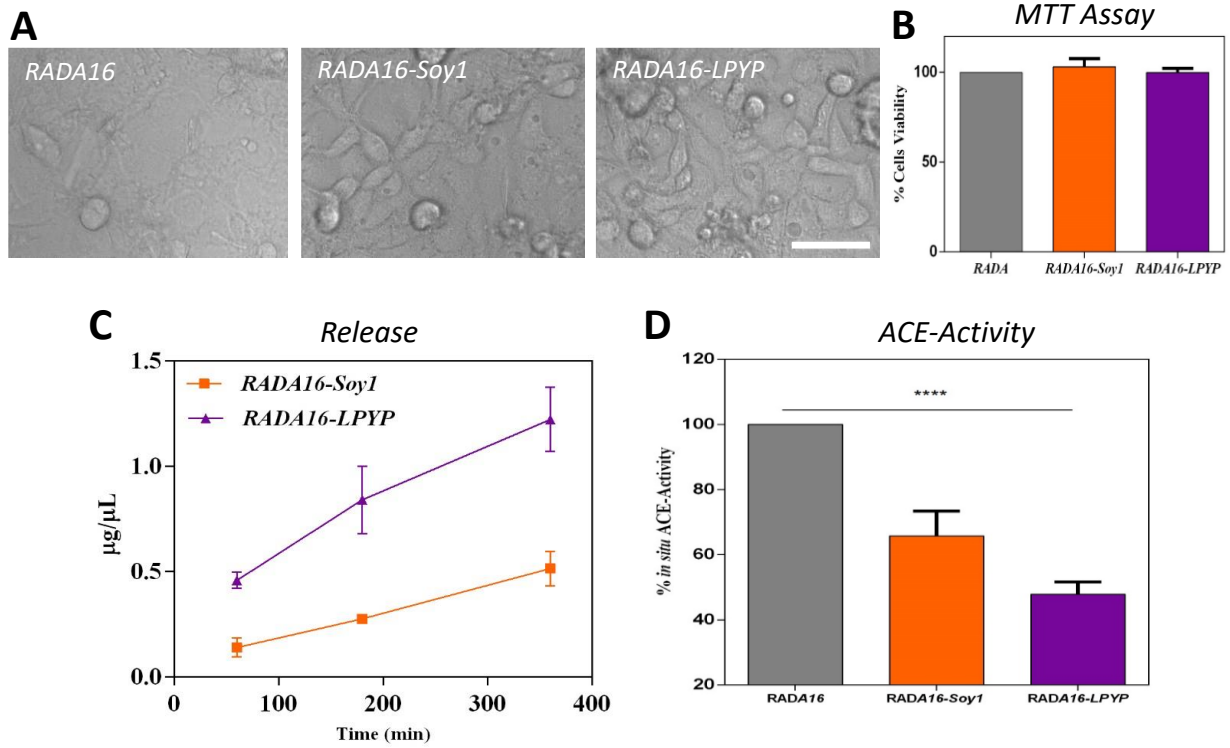
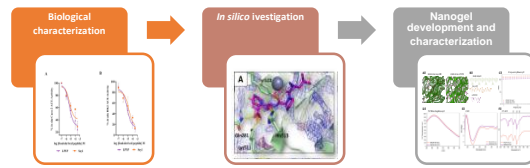


Figure 5



TOC